

Raman spectra of semiconductor nanoparticles: Disorder-activated phonons

Alka Ingale and K. C. Rustagi

Centre for Advanced Technology, Indore 452013, India

(Received 24 March 1998)

We present Raman spectra of four semiconductor doped glasses and a single crystal of $\text{CdS}_{0.55}\text{Se}_{0.45}$ in the range $30\text{--}800\text{ cm}^{-1}$ in the backscattering geometry. This includes the first-order Raman scattering from the disorder-activated zone-edge phonons and the LO phonons. TO phonon modes are not observed, as in bulk CdS, for the excitation well above the lowest gap. We show that the asymmetric line profile of the LO phonon structure can be understood as a composite of two phonon modes: the zone center and the zone edge phonons. Disorder-activated modes in the $(30\text{--}130)\text{-cm}^{-1}$ range and the higher-order Raman spectra are also observed and found to be consistent with this assignment. [S0163-1829(98)04235-0]

I. INTRODUCTION

The size dependence of electronic and vibrational spectra and of the electron-phonon interaction in semiconductor nanoparticles is important for a basic understanding of these materials as well as for establishing their potential optoelectronic applications. In this context Raman spectra of semiconductor nanoparticles have been investigated from several different angles in recent years.^{1–10} The low-frequency Raman spectra attributed to confined acoustic phonons have been used as a convenient means of determining the particle size.^{2,5} The other important aspect is the asymmetric broadening of the LO phonon lines and has variously been interpreted as due to confinement-induced relaxation of the $q \approx 0$ selection rule⁷ or the occurrence of a surface phonon.⁸ On the other hand, it is well known that the Raman spectra of mixed semiconductors such as $\text{Al}_x\text{Ga}_{1-x}\text{As}$,^{11,12} $\text{CdS}_x\text{Se}_{1-x}$,¹³ $\text{CdZn}_x\text{Te}_{1-x}$,¹⁴ and $\text{InGa}_x\text{As}_{1-x}$ (Ref. 15) also show asymmetric LO and TO phonon modes even in the bulk state. Various mechanisms invoked to explain this asymmetry include the Fano-like line shape due to the interaction between the LO phonon and the disorder-activated phonon continuum, the limited phonon correlation length due to lattice disorder, and a model in which the main effect of disorder is taken to be a disorder-induced scattering from the zone-edge phonon. Using time-resolved Raman scattering from nonequilibrium phonons with well-defined wave vectors, Kash *et al.*¹⁶ had concluded that in $\text{Al}_{0.11}\text{Ga}_{0.89}\text{As}$ the GaAs phonon wave vector remains well defined and the phonons are not localized on the $(0\text{--}100)\text{-nm}$ scale. This implies that in these systems the asymmetry of the phonon line shape cannot be attributed to the finite correlation length of phonons. However, in the small particles with sizes of the order of 10 nm, the phonons are expected to be localized within this range and all the above mechanisms could also contribute to the asymmetry of the line shape. To obtain a clearer understanding of the relative importance of finite-size effects and disorder in semiconductor nanoparticles, we have measured the Raman spectra of several semiconductor-doped glasses (SDG's) as well as that of a single crystal of $\text{CdS}_x\text{Se}_{1-x}$. Our results show that the disorder-induced zone-edge phonon Raman scattering plays an important role in SDG's also. Higher-order Raman spectra and other disorder-activated structures are also observed and found to be well understood in this picture.

In Sec. II we describe our samples and present our experimental spectra. These are analyzed in Secs. III and IV. In Sec. III the observed spectrum of a $\text{CdS}_x\text{Se}_{1-x}$ mixed crystal is analyzed. As expected, a two-mode behavior is seen in the Raman spectrum. The line shape of the CdSe-like LO mode at $\approx 200\text{ cm}^{-1}$ and the CdS-like LO mode at $\approx 300\text{ cm}^{-1}$ are shown to be best described by adding the contribution of the disordered-induced zone-edge phonon. Earlier, disordered-induced zone-edge optical phonons has been observed by Kash *et al.*¹⁶ and by Leng *et al.*¹¹ for $\text{Al}_x\text{Ga}_{1-x}\text{As}$. In Sec. IV we analyze the first-order Raman spectra of SDG's containing $\text{CdS}_x\text{Se}_{1-x}$ nanoparticles. We show that the LO phonon line shapes in SDG's are again best described in terms of a composite of two Lorentzian peaks, one corresponding to a $q=0$, LO phonon and the other corresponding to a zone-edge-LO (ZE-LO) phonon. Even in the sample RG715, which shows no CdS-like mode, as it is supposed to contain almost pure CdSe nanoparticles, the small sulphur content in the sample manifests itself as a local mode on the higher-frequency side and contributes to the activation of zone-edge-LO phonon. In Sec. V we present spectroscopic and other corroborative arguments to show that the second mode is better described as the ZE-LO phonon rather than a surface phonon mode. All our spectra are recorded with photon energies well above the band gap, which ensures similar scattering mechanisms to play important roles for SDG's and the $\text{CdS}_x\text{Se}_{1-x}$ single crystal. Since well above the band edge the density of states does not have any sharp features; quantum size effects do not appear to be important, except perhaps in determining the fluorescence spectra. Our conclusions are summarized in Sec. VI.

II. EXPERIMENTAL DETAILS

The SDG's are borosilicate glasses doped with $\leq 1\%$ by volume of $\text{CdS}_x\text{Se}_{1-x}$ nanocrystallites of diameter $\leq 100\text{ Å}$. Most of the earlier studies have concentrated on confinement effect for optical phonons. Keeping this in mind, we have selected four Schott color glass filters OG515 ($x \sim 0.92$, $d \sim 56\text{ Å}$), OG530 ($x \sim 0.87$, $d \sim 56\text{ Å}$), OG590 ($x \sim 0.5$, $d \sim 60\text{ Å}$), and RG715 ($x \sim 0.0$, $d \sim 110\text{ Å}$) (Ref. 17) covering a wide range of composition and size and a $\text{CdS}_x\text{Se}_{1-x}$ ($x = 0.55$) single crystal for our studies. First- and second-order unpolarized Raman spectra of all these samples were recorded in the backscattering geometry. $\text{CdS}_x\text{Se}_{1-x}$ crystal

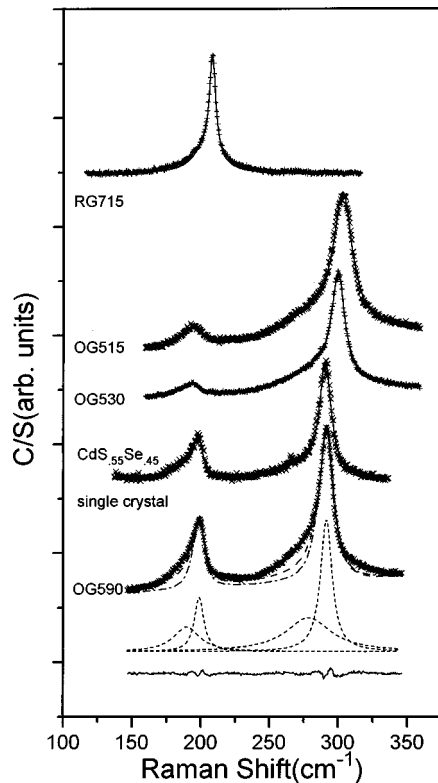


FIG. 1. Raman spectra of the Schott filter OG590, the $\text{CdS}_{0.55}\text{Se}_{0.45}$ single crystal, and the Schott filters OG530, OG515, and RG715. Experimental points for the Schott filter OG590 are shown by crosses. The three theoretical fits are shown by short dashes for the SCM, long dashes for the Fano profile, and a solid line for the two-Lorentzian fit. For OG590 individual Lorentzians corresponding to an additional phonon and LO ($q=0$) phonon obtained in the two-Lorentzian fit are shown below by short dashes. The difference between the experimental and calculated line shapes for the two-Lorentzian fit is shown at the bottom by the solid line.

was polished using $0.05\text{-}\mu\text{m}$ alumina powder. The absorption edge obtained from the absorption data taken on a spectrophotometer (Shimadzu UV3101PC) at room temperature (RT) is 630 nm . For $\text{CdS}_x\text{Se}_{1-x}$ the composition dependence of the band gap $E_g(x)$ at RT is given by¹⁸

$$E_g(x) = 1.7 + 0.17x + 0.55x^2. \quad (1)$$

This gives x as ≈ 0.55 . The $\text{CdS}_x\text{Se}_{1-x}$ crystal has a hexagonal structure. The x-ray diffraction and birefringence measurements indicate that for our sample the C axis is at about $76^\circ \pm 2^\circ$ to the normal to the front plane.

The Raman spectra were excited at RT by a line focus ($\approx 3\text{ mm} \times 50\text{ }\mu\text{m}$) of Ar-ion laser excitation at 4579 and $5145\text{ }\text{\AA}$ to achieve a reasonable signal-to-noise ratio in each case. The backscattered light was passed through a double monochromator (Jobin Yvon Model No. U1000) and detected by a photomultiplier tube (Hamamtsu Model No. R943-02) in the photon counting mode. The resolution of spectrometer was $\approx 2\text{ cm}^{-1}$. The frequencies obtained for LO modes in all SDG's are consistent with known composition and earlier Raman data on $\text{CdS}_x\text{Se}_{1-x}$.^{9,13} As shown in Fig. 1, two LO modes were observed in the samples OG515, OG530, and OG590: one was a CdSe-like mode at $\approx 200\text{ cm}^{-1}$ and the other was a CdS-like mode at $\approx 300\text{ cm}^{-1}$. In

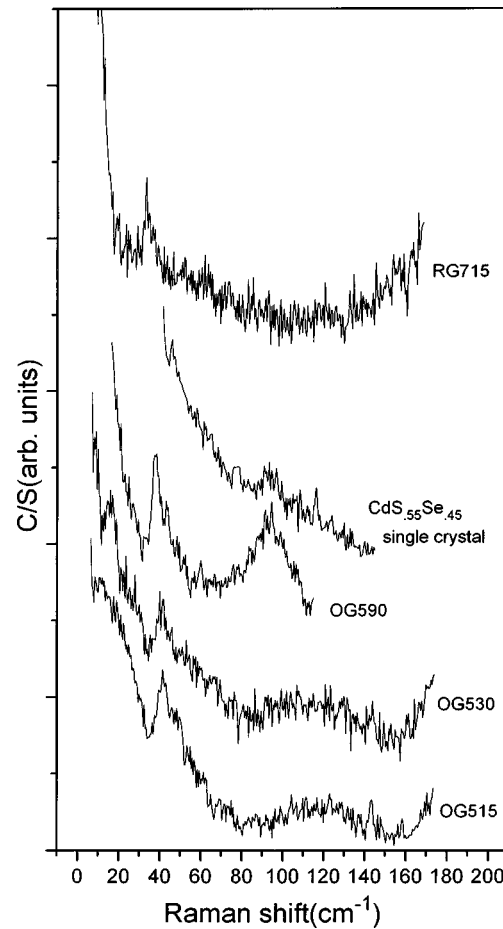


FIG. 2. The $(20\text{--}120)\text{-cm}^{-1}$ region of the Raman spectra for OG515, OG530, OG590, and RG715 showing confined acoustic phonons and disorder activated spectra.

the sample RG715 only the CdSe-like mode is observed, which is consistent with the fact that this sample contains crystallites of almost pure CdSe.

Raman spectra for all samples in the region $5\text{--}120\text{ cm}^{-1}$ (Fig. 2) showing confined acoustic phonons and disorder activated modes were also recorded in the backscattering geometry. Fluorescence was recorded to check the background of first-order Raman spectra. We have shown earlier that the low-frequency Raman spectra of confined acoustic phonons used for the size determination of the nanocrystal can be substantially improved when several samples are studied together.¹⁹

III. MIXED CRYSTAL

A mixed crystal of $\text{CdS}_x\text{Se}_{1-x}$ is expected to show two-mode behavior, i.e., two TO and two LO phonons should be observed in a single crystal, TO_1 and LO_1 corresponding to CdS-like optical phonons and TO_2 and LO_2 corresponding to CdSe-like optical phonons. The frequency, width, and line shape of optical phonons vary with composition.^{11–15} Two LO modes, as shown in Fig. 1, one CdSe like at 197 cm^{-1} and the other CdS-like at 290 cm^{-1} , were observed in the first-order Raman spectrum of this sample. These frequencies match well with the composition dependence of frequencies observed earlier by Tu and Persans.⁹ We note that although selection rules in the present configuration allow both the LO

and TO modes, we observe only LO modes. These are the “forbidden” LO modes, which become allowed near resonance.^{20,21} A major contribution to Raman scattering in this case comes from the q -dependent intraband Fröhlich term. Since this contributes only to LO modes, only LO modes are observed in such situations. This kind of behavior has been observed earlier for a CdS single crystal, where the Raman spectrum is excited with laser photon energies much higher than the fundamental gap that takes electrons deep in conduction band.²¹

The line profiles of the LO phonons, shown in Fig. 1, are clearly asymmetric. This asymmetry in line shapes has been observed earlier in many III-V and II-VI mixed semiconductors.^{11–15} For a quantitative description of this asymmetry it is important to treat any frequency-dependent background carefully. We use a spectral dependence of the kind $A + B\omega$ to account for the background due to the Rayleigh wing and fluorescence. The parameters A and B are calculated from the data away from LO modes and are kept the same for all models used for the calculation of the line profile.

The best fits to the line shape were obtained using the spatial correlation model (SCM) and Fano line-shape function as well as the model in which each peak is decomposed into two Lorentzians. In the SCM, the Gaussian correlation function⁷ with an isotropic cosine dispersion curve was used, i.e.,

$$\omega(q) = \omega_0 - \Delta\omega \sin^2\left(\frac{q}{q_z}\right), \quad (2)$$

where q_z is the sperical zone-edge wave vector and $\Delta\omega$ the dispersion width of the phonon branch. The best fit to the experimental data obtained for the correlation length $L = 80$ Å. In mixed crystals, the anharmonic interaction of the LO phonon with a continuum of other phonons may lead to an asymmetric Fano profile.^{12,14} In the two-Lorentzian model each LO structure has been fitted with two Lorentzians, i.e., the Raman intensity in this case is given by

$$I(\omega) = \sum_j \frac{S_j \Gamma_j}{(\omega - \omega_j)^2 + \Gamma_j^2}, \quad (3)$$

where ω_j denotes the frequency, Γ_j the half-width at half maximum (HWHM) and S_j the oscillator strength of the mode. The best fit to the experimental spectrum is obtained by the two-Lorentzian model. Quantitatively, we obtain $\chi^2 = 0.3$ for the two Lorentzian model, whereas for the SCM and Fano profile model χ^2 is 2.2 and 1.6, respectively.

It seems appropriate to examine here the origin of the second Lorentzian peak in mixed crystals, where no surface phonon exists. As mentioned earlier, near resonance the main contribution to Raman scattering is from the intraband Fröhlich interaction, with the cross section increasing linearly with q .²⁰ The nonzero value of q can arise from the small wave vector of the excitation source or from inhomogeneity over sizes smaller than the wavelength of light such as those due to large absorption, surface-field-induced scattering, or substitutional disorder. In mixed crystals, we expect the coexistence of two types of Raman spectra: (i) relatively narrow peaks at LO and TO phonon frequencies of the mixed crystal, obeying the usual Raman selection rules, and

(ii) broad, disorder-activated spectral features associated with phonon density of states.²² For the latter, the contribution of zone-edge phonons would dominate because of the larger density of states²³ and the q dependence of the intraband Fröhlich interaction for excitation well above the band edge. This analysis of the LO phonon line shape is consistent with and supports the earlier observations of Kash *et al.* based on time-resolved Raman spectroscopy.¹⁶

IV. LO PHONON LINE SHAPE IN SEMICONDUCTOR DOPED GLASSES

In SDG's the phonons are necessarily confined to dimensions of the order of the nanocrystal. The observed asymmetry of LO phonon structures can therefore be attributed to phonon confinement leading to contribution from $q \neq 0$ phonons, in addition to $q \approx 0$ phonon. In the SCM the best fit to the experimental data is obtained with a Gaussian function with a value of $\exp(-4\pi^2)$ at the boundary of nanocrystal.⁷ Following the same procedure as for the crystal, the LO phonon line shape was calculated for $\text{CdS}_x\text{Se}_{1-x}$ nanocrystals, except that the HWHM used now refers to the width of the phonon in the corresponding bulk material, i.e., the mixed crystal, and the correlation length L is replaced by d ,¹⁷ the average diameter of the nanocrystallites in the sample. The calculated line profiles for OG590 are shown in Fig. 1 for SCM by short dashes, the Fano profile by long dashes, and the two-Lorentzian fit by a solid line. The difference between the experimental data and the calculated line shape in the two-Lorentzian model is shown at the bottom by a solid line. It is very small and structureless. The least-squares fit parameters for the two-Lorentzian model for SDG's are given in Table I. It is appropriate to note here that the excitation wavelength used for the crystal and SDG's is such that the electron is excited deep into the conduction band. Therefore, one expects similar resonance scattering mechanisms to be important in both the cases. Figure 1 also shows the two Lorentzians obtained for each LO mode from the two-Lorentzian model fit for the sample OG590.

As in the single crystal, the background of the type $A + B\omega$ for each sample is used for the fitting in all the models. The background in the Raman spectra of SDG's is mainly due to fluorescence and the background parameters obtained for different samples represent this suitably. From fluorescence data, it is also clear that for the single crystal, the band-edge fluorescence goes down quickly to zero above the band gap, as expected. Hence the contribution to the background here is only from the Rayleigh wing. We should note that even if the particle diameter or the background parameters are allowed to vary, the best fit remains that given by the two-Lorentzian model as for the crystal. However, if the parameters describing the background are allowed to vary freely, a comparable fit can be obtained in the Fano profile model also, but the corresponding parameters for the background turn out to be unphysical.

The χ^2 obtained in the SCM and Fano profile is ≈ 2 – 4 , whereas for the two-Lorentzian fit it is ≈ 0.3 – 0.5 for all SDG's. This shows that even if a small asymmetry is introduced, as described by the SCM, due to confinement of the phonon in the nanocrystal and or the Fano profile due to the interaction with the disorder-activated continuum, a major

TABLE I. Parameters obtained for best fit for all samples using two Lorentzian models.

Sample	ZE-LO ₁			LO ₁			ZE-LO ₂			LO ₂		
	ω (cm ⁻¹)	Γ (cm ⁻¹)	S	ω (cm ⁻¹)	Γ (cm ⁻¹)	S	ω (cm ⁻¹)	Γ (cm ⁻¹)	S	ω (cm ⁻¹)	Γ (cm ⁻¹)	S
OG515	283	26	5625	303	8	9839	184	12	553	194	7.2	1122
OG530	287	26	6163	299	5.4	5007	185	12	560	193	5.6	507
Crystal	271	18	802	290	5.2	1768	188	9.4	472	197	5.2	418
OG590	278	19	8253	291	5	8175	189	11	3501	198	4.2	2772
RG715							203	11	1256	208	2.73	1238

contribution to the asymmetry is from the contribution of an additional phonon mode on the low-frequency side of the LO ($q=0$) phonon. We note here that χ^2 obtained for the SCM and Fano profile is larger for the SDG's than for the single crystal, i.e., the additional mode is more prominent in SDG's. This, we believe, is due to additional disorder in SDG's, indicated, for example, by the large number of traps present in them, which gives rise to a large and higher-wavelength side of the band-edge fluorescence due to traps. This feature is absent in crystal fluorescence data at RT.

V. NATURE OF THE ADDITIONAL MODE

The additional mode invoked in the two-Lorentzian model in SDG's could be attributed to the zone-edge LO phonon or the surface phonon mode. The strongest argument for this additional phonon to be a ZE-LO phonon is that it is also observed in the CdS_{0.55}Se_{0.45} single crystal. The sample RG715 is known to be composed of pure CdSe with trace amounts of sulphur⁶ and thus provides a special test case in that one could expect the finite-size effects to be dominant. Here the CdSe-like mode is relatively sharp with a HWHM of about 2.7 cm⁻¹ (≈ 2.1 cm⁻¹ after correcting for an instrumental resolution of 2 cm⁻¹) compared to the value of more than 5 cm⁻¹ in all other cases. However, even in this case the two-Lorentzian model provides a much better fit and the asymmetry and broadening could be attributed to the disorder-activated ZE-LO₂ phonon. In the following we present other corroborative observations and a calculation showing a better spectroscopic description of this additional phonon as a ZE-LO phonon than as a surface phonon.

We first look at the frequencies of various modes in our samples as a function of composition. In a two-mode mixed crystal, the nature of vibrational modes changes with concentration. In a S-rich sample of CdS_xSe_{1-x}, a CdS-like mode would be expected to propagate but a CdSe-like mode would be more like a gap mode with an amplitude of vibration decaying away from the impurity atom. In a nanocrystal this distinction gets blurred if the phonon correlation length is larger than the size of the nanoparticle. The CdSe-like modes in S-rich samples OG515 and OG530, in fact, can be reasonably well described by a single Lorentzian, although quite broad. For these samples the CdS-like LO modes can be taken as propagating modes. In this case a "random element isodisplacement" model description of phonons is appropriate and the second Lorentzian in the LO phonon structure can be assigned to the ZE-LO phonon.²⁴ To estimate the frequencies of the LO modes in mixed crystals, we start with

TO mode frequencies of CdS-like and CdSe-like phonons, which vary nearly linearly with concentration x as^{25,26}

$$\begin{aligned}\omega_{\text{TO}_1} &= 266 - 28x \text{ cm}^{-1}, \\ \omega_{\text{TO}_2} &= 168 + 17x \text{ cm}^{-1}.\end{aligned}\tag{4}$$

For $x=0.0$, the TO₁ frequency corresponds to that of the local mode of S in CdSe and the TO₂ corresponds to the TO phonon of CdSe. Similarly for $x=1$, the TO₁ frequency corresponds to the TO phonon of CdS and TO₂ corresponds to that of the gap mode of Se in CdS.

For CdS and CdSe, we have nonoverlapping restrahlen bands and it is a good approximation to write the dielectric response function of the CdS_xSe_{1-x} mixed crystal as

$$\epsilon(\omega) = x\epsilon_1(\omega) + (1-x)\epsilon_2(\omega),\tag{5}$$

where the subscripts 1 and 2 refer to CdS and CdSe, respectively. The two LO mode frequencies are solutions of the equation $\epsilon(\omega)=0$, which can be written as

$$\begin{aligned}\epsilon(\infty)\omega^4 - \omega^2[\epsilon(\infty)(\omega_{\text{TO}_1}^2 + \omega_{\text{TO}_2}^2) + xS_1\omega_{\text{TO}_1}^2 \\ + (1-x)S_2\omega_{\text{TO}_2}^2] + \omega_{\text{TO}_1}^2\omega_{\text{TO}_2}^2[\epsilon(\infty) + xS_1 + (1-x)S_2] \\ = 0,\end{aligned}\tag{6}$$

with S_1, S_2 and $\omega_{\text{TO}_1}, \omega_{\text{TO}_2}$ denoting the oscillator strength and composition-dependent TO mode frequencies for CdS- and CdSe-like modes for x . The small concentration dependence of S_1, S_2 is neglected and these are taken to be the oscillator strengths for the end members CdS and CdSe, respectively. For CdS and CdSe individually, the oscillator strength $S = \epsilon_0 - \epsilon_\infty$ is given by the Lyddane-Zachs-Teller relation as

$$(\omega_{\text{LO}}^2 - \omega_{\text{TO}}^2)/\omega_{\text{TO}}^2 = S/\epsilon_\infty.\tag{7}$$

Consistently with Eq. (5), $\epsilon(\infty)$ in Eq. (6) is taken to be the weighted average of the electronic dielectric functions of CdS and CdSe, where $\omega_{\text{LO}}=302$ cm⁻¹ for CdS and 210 cm⁻¹ for CdSe and $\epsilon_\infty=5.32$ for CdS and 6.1 for CdSe.²⁷ Using these parameters, Eqs. (4) and (6) yield the variation of ω_{LO_1} , ω_{LO_2} , ω_{TO_1} , and ω_{TO_2} as a function of x , as shown in Fig. 3.

From an earlier pressure dependence study of impurity-induced modes in CdS and available dispersion curves for CdS, the ZE-LO phonon (at K or L critical points) is esti-

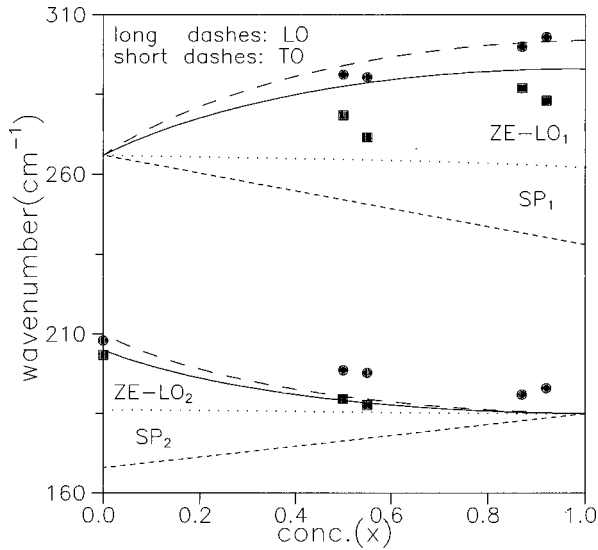


FIG. 3. Calculated concentration dependence of frequencies of LO (long dashes) and TO (short dashes) phonons for both CdS- and CdSe-like modes in a mixed crystal of $\text{CdS}_x\text{Se}_{1-x}$. The variation of ZE-LO modes as a function of x is shown by solid line. The observed zone center LO and ZE-LO mode frequencies as listed in Table I are plotted as solid circles and solid squares, respectively. The calculated surface phonon frequencies for $l=1$ and $n=0$ are shown by dots.

mated to have a frequency $\approx 293 \text{ cm}^{-1}$.^{13,23} Dispersion curves for CdSe are not available in the literature, but owing to the fact that the crystalline structure, the effective charge, and the spring constants are nearly the same in CdSe, it is reasonable to assume that the CdSe dispersion curve is similar to that of CdS, scaled to lower energies. The scaling relation is given by¹³

$$\frac{\omega_0(\text{CdSe})}{\omega_0(\text{CdS})} = \sqrt{\frac{2\omega_{\text{TO}}^2(\text{CdSe}) + \omega_{\text{LO}}^2(\text{CdSe})}{2\omega_{\text{TO}}^2(\text{CdS}) + \omega_{\text{LO}}^2(\text{CdS})}}. \quad (8)$$

The frequency of the ZE-LO₂ phonon for CdSe is estimated to be 205.4 cm^{-1} . This compares well with second Lorentzian peak at 202.7 cm^{-1} for the sample RG715, taking into account the observed redshift by $\approx 2 \text{ cm}^{-1}$ of the zone-center LO₂ mode frequency relative to the bulk value. As $x \rightarrow 0$, the frequency of the ZE-LO₁, CdS-like phonon should also go to the local mode frequency of S in CdSe. We interpolate the frequency difference $\omega_{\text{LO}_1} - \omega_{\text{ZE-LO}_1}$ linearly with x . The composition dependence of $\omega_{\text{ZE-LO}_1}$ obtained in this way is shown in Fig. 3 by a solid line and is quite similar to that found by Leng *et al.*¹¹ using a one-dimensional chain model. Similarly, the $\omega_{\text{ZE-LO}_2}$ frequency for the CdSe-like mode is calculated and is shown by a solid line in Fig. 3.

As mentioned earlier, the additional phonon in the LO phonon structure has been attributed to surface phonon by Mlayah *et al.*⁸ In a spherical crystal of diameter d , surrounded by a medium having a real, frequency-independent dielectric constant ϵ_m , surface mode frequencies lie between transverse and longitudinal bulk modes.²⁹ The surface phonon with $n=0$ and $l=1$ is the first of the series of surface phonon modes. It has uniform polarization over the whole volume and is expected to have the largest Raman cross

section.²⁹ These Fröhlich mode frequencies corresponds to $-\epsilon(\omega) = \epsilon_m^l \equiv \epsilon_m(l+1)/l$, where ϵ_m is the dielectric constant of the host medium in the infrared range. Frequencies of surface phonon are given by solutions of the equation

$$\omega^4 + \omega^2[\omega_{T1}^2 + x(\omega_{l1}^2 - \omega_{T1}^2) + \omega_{T2}^2 + (1-x)(\omega_{l2}^2 - \omega_{T2}^2)] + \omega_{T1}^2\omega_{T2}^2 \left[1 + x \frac{\omega_{l1}^2 - \omega_{T1}^2}{\omega_{T1}^2} + (1-x) \frac{\omega_{l2}^2 - \omega_{T2}^2}{\omega_{T2}^2} \right] = 0, \quad (9)$$

where

$$\frac{\omega_{l1}^2 - \omega_{T1}^2}{\omega_{T1}^2} = \frac{S_1}{\epsilon_\infty^1 + \epsilon_m^{(l)}}. \quad (10)$$

Frequencies for the surface phonon mode ($n=0, l=1$) were calculated as a function of x and are shown in Fig. 3 by dots. We take the dielectric constant of the medium to be $\epsilon_m = 4.64$.²⁸

The observed and calculated mode frequencies are shown together in Fig. 3. The observed LO₁ mode frequencies lie consistently lower than the theoretical estimates. The LO₂ mode frequencies lie consistently higher than values predicted by theory. This discrepancy may be partly due to the inadequacy of the theory²⁴ and partly due to finite-size and stress effects in nanocrystals.^{4,7,10} No finite-size effects are taken into account in the above frequency calculations. Nevertheless, it is clear that the second Lorentzian peak frequency for LO₁ and LO₂ structures is better described by the ZE-LO phonon variation than the surface phonon variation as a function of composition. It is interesting to note here that in RG715, as shown in Fig. 4, a weak structure is observed near 268 cm^{-1} . We believe that this is a local mode due to a small S concentration in CdSe.^{13,24} This observation supports the occurrence of the ZE-LO phonon mode in the Raman spectrum of RG715; however, S is not essential for disorder. These results suggest that the intensity of the second Lorentzian could be taken as a measure of the departure from perfect crystalline order in nanoparticles.

At this point we note that the observed LO phonon, leading to the second Lorentzian, is not observed generally in III-V mixed semiconductors. The reason is twofold. One is that the effective charge of the optical phonon for III-V semiconductors is small compared to that of II-VI and the cross section of the disorder-induced ZE optical phonon will be large for II-VI compounds, as the Fröhlich interaction is directly proportional to the effective charge. The intensity, however, depends on disorder. The other important reason is that, although ZE optical phonons are observed in III-V mixed crystals due to disorder, the related frequencies lie much higher than the zone-center TO phonon and much below the LO phonon,²³ leading to separate structures in the spectra as discussed below.

The disorder-activated zone-edge LO, TO, TA, and LA phonon modes have been observed earlier in several semiconductor mixed crystals.^{11–15,22} The most studied example is that of $\text{Al}_x\text{Ga}_{1-x}\text{As}$. In molecular-beam epitaxy grown $\text{Al}_x\text{Ga}_{1-x}\text{As}$, very good agreement has been obtained between calculated and experimental phonon frequencies for several modes including disorder-activated optical modes for

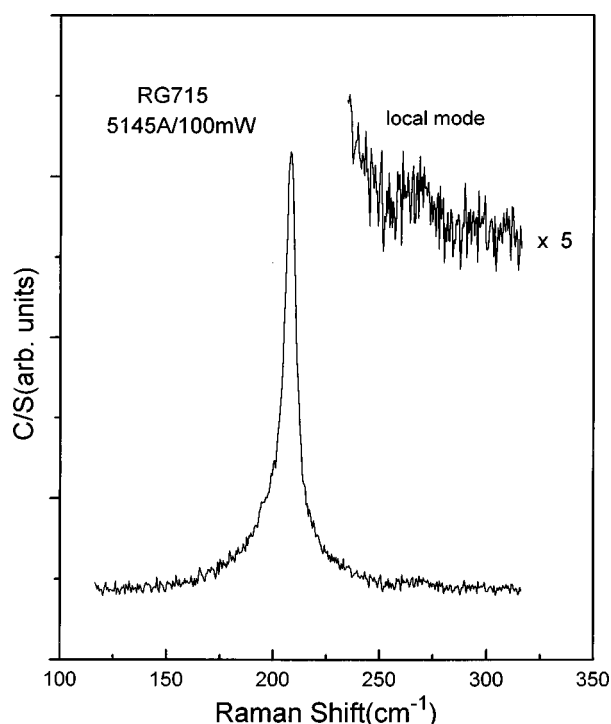


FIG. 4. Raman spectrum showing the local mode in the CdSe-rich Schott filter RG715. The inset shows the local mode at 268 cm^{-1} due to the small S concentration in this sample.

the entire range $x=0-1$.¹¹ The calculation of phonon frequencies using a simple chain model shows this to be the ZE-LO phonon at the X point. Similarly, for $\text{InGa}_x\text{As}_{1-x}$ ($x \approx 0.5$) a recent line shape analysis by Estrera *et al.*¹⁵ of Raman spectra in different configurations revealed the existence of an additional disorder-activated mode denoted by R^* , which lies below the TO and the LO ($q=0$) GaAs-like phonons. From dispersion curves of GaAs and InAs, we can correlate this mode to be the GaAs-like ZE-TO mode.²³ With a linear composition dependence of the ZE-TO phonon frequency it is estimated to be $\approx 243.5\text{ cm}^{-1}$ for $x=0.5$, whereas the R^* mode occurs at 244 cm^{-1} . The ZE-LO mode is not observed in this case, presumably due to the much smaller density of states.²³

Apart from frequency, Hayashi and Yamamoto³⁰ have noted that for the surface, the phonon mode shifts to lower frequencies as the dielectric constant ϵ_m of the surrounding medium increases and it becomes stronger as the size of the particle reduces. The surface phonon is not sensitive to compositional disorder. Experimentally, however, the line shapes of the LO phonons of CdS and CdSe nanoparticles of various sizes in the GeO_2 matrix from Tanaka, Onari, and Arai¹⁰ show a much smaller asymmetry and are well described by the spatial correlation model, indicating a negligibly small contribution from the surface phonon. Further, with the reduction in size the anticipated increase in the strength of the surface phonon is not observed in our samples, where the diameter varies from 110 to 56 \AA , nor in the work of Tanaka, Onari, and Arai,¹⁰ where sizes vary from 100 to 16 \AA for both CdS and CdSe particles. In addition, the width of this additional phonon is large, $\approx 35-50\text{ cm}^{-1}$, whereas for the surface phonon it is expected to be the same as that of the bulk LO phonon.²⁹ In nanocrystals the LO phonon width may increase due to the size distribution as the LO frequency

depends on the size of the nanocrystal. However, the surface phonon frequency does not depend on size and therefore the size distribution should not increase the width of the surface phonon. The width of the surface phonon is therefore expected to be $\approx 3-4\text{ cm}^{-1}$. In an earlier observation of unambiguously identified surface phonons in other materials, the width was larger than that of the bulk phonon by 4–5 times,³⁰ but still much smaller than that observed here, i.e., $\approx 35-50\text{ cm}^{-1}$.

We also looked for additional disorder-activated structures in the region $30-130\text{ cm}^{-1}$ (Fig. 2) to seek further support for the view that this additional phonon is the disorder-activated ZE-LO phonon. As shown in Fig. 2, two prominent structures are observed, one structure in the region $30-55\text{ cm}^{-1}$ and the other broader structure in the region $85-130\text{ cm}^{-1}$ for all the samples except RG715, where the latter is not clearly observed. The peak at about 45 cm^{-1} in S -rich samples OG515 and OG530, which shifts towards 33 cm^{-1} for the Se -rich sample, is attributed to $ZE-E_2(\text{TO})$ (CdS-like) phonons from the dispersion curve of CdS and an appropriate scaling down of frequencies for CdSe.²³ This mode can also be attributed to the $E_2(q=0)$ (CdS-like) mode purely on the basis of frequency, as the dispersion of the E_2 mode is very small.²³ However, in that case it should have a Lorentzian line shape, even if the confinement effect is taken into account. In contrast, as one can see from Fig. 2, this mode has a shoulder on the higher-frequency side in all the samples. We attribute this to the presence of an additional mode corresponding to the ZE-LA phonon. In fact, this additional mode is clearly observed as a separate peak for OG515 and OG590. The other structure in the region $85-130\text{ cm}^{-1}$ has been assigned earlier to $LO_1\text{-}LO_2$ for OG590.^{2(b)} However, the Raman spectra of all these samples together reveal a more interesting story. This structure lies higher than the corresponding $LO_1\text{-}LO_2$ frequency for OG515 and OG530 by 10 and 7 cm^{-1} , respectively. In addition, the width of the structure reduces from OG530 to OG590 and the single crystal. This observations can be explained qualitatively if we take this broad structure to be a composite of two modes, one $LO_1\text{-}LO_2$ and the other the higher-frequency $ZE-E_2(\text{LO})$ (CdS-like) mode.²³ The frequencies of the $LO_1\text{-}LO_2$ and $ZE-E_2(\text{LO})$ (CdS-like) modes both decrease with decreasing sulphur content, but the $ZE-E_2(\text{LO})$ (CdS-like) mode decreases much faster. This manifests in the largest width of this mode, at the highest S concentration as the two modes are farthest from each other, whereas in OG590 the $LO_1\text{-}LO_2$ and $ZE-E_2(\text{LO})$ (CdS-like) modes may be closer, giving a pronounced peak of much smaller width for OG590. We also note that in Fig. 2 an additional phonon density of states can be seen between 45 and 90 cm^{-1} for all the samples, as expected for disordered systems.

Higher-order Raman spectrum

In the higher-order spectrum of these samples, combination phonons $2LO_2$, LO_1+LO_2 , $2LO_1$, and $3LO_1$ and difference phonons $3LO_1\text{-}LO_2$ and $LO_1\text{-}LO_2$ are observed. Figure 5 shows the first- and higher-order spectra of OG590. In view of the observation of the ZE-LO phonon in the first-order spectrum, the broad structures corresponding to $2LO_2$

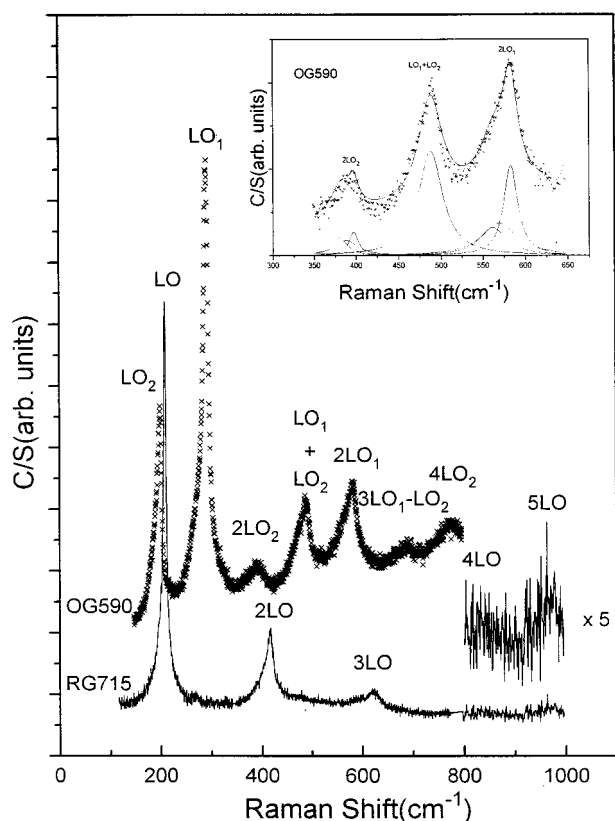


FIG. 5. Higher-order Raman spectra of the Schott filters RG715 and OG590. The inset shows the second-order Raman spectrum of OG590 as crosses along with the seven Lorentzian fit corresponding to $2ZE-LO_2$, $ZE-LO_2+LO_2$, $2LO_2$, LO_1+LO_2 , $2ZE-LO_1$, $ZE-LO_1+LO_1$, and $2LO_1$ as a solid line. The separate Lorentzians are shown by solid lines.

and $2LO_1$ were fitted with three Lorentzians each, with the first corresponding to the $2ZE-LO$ mode, the second corresponding to the $ZE-LO+LO$ mode, and the third corresponding to the $2LO$ mode. Using the frequencies obtained for $ZE-LO$ and LO mode frequencies from the least-squares fits of the first-order spectra, a satisfactory fit to the second-order spectrum is obtained for all the samples. The inset of Fig. 5 shows the corresponding fit for the sample OG590. The HWHM used for Lorentzians corresponding to $2ZE-LO$ and $ZE-LO+LO$ was about the same as that obtained for $ZE-LO$ in the first-order spectrum, whereas the HWHM used for the Lorentzian corresponding to $2LO$ was varied to obtain the best fit to the data and was found to be slightly higher than that of the LO mode in the first-order spectra. For the LO_1+LO_2 structure, we find that a satisfactory fit is obtained even without invoking the $ZE-LO_1+ZE-LO_2$ mode. The intensity of the LO_1+LO_2 mode is higher than that of the $2LO$ mode of the minority constituent as observed before.^{8,13} In

RG715, structures up to $5LO$ are observed, as shown in Fig. 5. Together, the results for higher-order spectra further support the presence of the $ZE-LO$ phonon in the first-order spectrum, which leads to the asymmetry of the LO phonon line shape.

VI. CONCLUSION

We have investigated the asymmetry of the LO phonon line shape in semiconductor doped glasses with differing composition of the mixed crystal. A comparison of the first- and second-order Raman spectra of single-crystal $CdS_{0.55}Se_{0.45}$ with those of SDG's reveals that the disorder-activated Raman spectrum is a major feature in all SDG's selected. Of all the well-known models, the best fit to the asymmetric line shape of the LO phonon has been obtained using a model that decomposes each such structure into two Lorentzians. This second phonon mode is sometimes attributed to the surface phonon. However, we assign it to be the zone-edge LO phonon, as this is observed also in the Raman spectrum of the $CdS_{0.55}Se_{0.45}$ single crystal. The observation of other disordered activated structures such as $ZE-E_2(LO)$, $ZE-E_2(TO)$, and $ZE-LA$ modes further supports this attribution. In contrast, the observation of the surface phonon would have been surprising since surface phonons were not observed by Tanaka, Onari, and Arai,¹⁰ in pure CdS and $CdSe$ quantum dots embedded in the GeO_2 matrix even with smaller diameter nanocrystals and earlier resonance studies of GaP quantum dots show that resonance enhancement of the LO mode is much larger than that of the surface phonon as one approaches the direct band gap.³¹

A recent calculation by Chamberlain, Trallero-Giner, and Cardona emphasizes the mixed nature of phonons (LO , TO , and surface phonon character) in quantum dots.³ The incoming and outgoing resonances are expected to result in dramatic changes in the Raman spectrum as a function of excitation frequency near the band edge. In all our considerations quantum size effects on electron spectra and optical phonons are neglected. We note that in our experimental situation, electrons are excited deep in the conduction band, where the electron density of states is nearly continuous and a bulklike treatment seems appropriate.

ACKNOWLEDGMENTS

We are indebted to Dr. M. J. Tafreshi, Anna University, Chennai for providing the $CdS_{0.55}Se_{0.45}$ single-crystal sample. We are grateful to Professor Ajay Sood, Dr. A. Roy, and K. S. Bindra for useful discussions. It is a pleasure to thank G. Jayaprakash and Surendra Singh for their technical assistance.

¹T. Bischoff, M. Iwanda, G. Lermann, A. Materny, W. Kiefer, and J. Kalus, *J. Raman Spectrosc.* **27**, 297 (1996), and references therein.

²(a) A. Roy and A. K. Sood, *Solid State Commun.* **97**, 97 (1996); (b) *Phys. Rev. B* **53**, 12 127 (1996).

³M. P. Chamberlain, C. Trallero-Giner, and M. Cardona, *Phys.*

Rev. B **51**, 1680 (1995), and references therein.

⁴V. Spagnolo, G. Scamarcio, M. Lugara, and G. C. Righini, *Superlattices Microstruct.* **16**, 51 (1994).

⁵B. Saviot, B. Champagnon, E. Duval, I. A. Kuriastev, and A. I. Ekimov, *J. Non-Cryst. Solids* **197**, 2789 (1996).

⁶M. C. Klien, F. Hache, D. Ricard, and C. Flytzanis, *Phys. Rev. B*

- 42**, 11 123 (1990), and references therein.
- ⁷J. H. Campbell and P. M. Fauchet, *Solid State Commun.* **58**, 739 (1986).
- ⁸A. Mlayah, A. M. Brugman, R. Carles, J. B. Renucci, M. Ya. Valakh, and A. V. Pogorelov, *Solid State Commun.* **90**, 567 (1994).
- ⁹A. Tu and P. D. Persans, *Appl. Phys. Lett.* **58**, 1506 (1991).
- ¹⁰A. Tanaka, S. Onari, and T. Arai, *J. Phys. Soc. Jpn.* **61**, 4222 (1992); *Phys. Rev. B* **45**, 6587 (1992).
- ¹¹J. Leng, Y. Qian, P. Chen, and A. Madhukar, *Solid State Commun.* **69**, 311 (1989).
- ¹²O. Brafman and R. Manor, *Phys. Rev. B* **51**, 6940 (1995).
- ¹³R. Beserman, *Solid State Commun.* **23**, 323 (1977).
- ¹⁴D. J. Olego, P. M. Raccach, and J. P. Faurie, *Phys. Rev. B* **33**, 3819 (1986).
- ¹⁵J. P. Estrera, P. D. Stevens, R. Glosser, W. M. Duncan, Y. C. Kao, H. Y. Liu, and E. A. Beam III, *Appl. Phys. Lett.* **61**, 1927 (1992).
- ¹⁶J. A. Kash, J. M. Hvam, J. C. Tsang, and T. F. Kucch, *Phys. Rev. B* **28**, 5776 (1988).
- ¹⁷G. P. Banfi and V. Degiorgio, *J. Appl. Phys.* **74**, 6925 (1993).
- ¹⁸A. A. I. Al-Bassam and A. M. Al-Dhafiri, *J. Cryst. Growth* **134**, 63 (1993).
- ¹⁹Alka Ingale, in *Physics of Semiconductor Nanostructures*, edited by K. P. Jain (Narosa Publishing, New Delhi, 1997).
- ²⁰M. Cardona, in *Light Scattering in Solids II*, edited by M. Cardona and G. Guntherodt (Springer, Heidelberg, 1982), p. 19.
- ²¹M. V. Klein and S. P. S. Porto, *Phys. Rev. Lett.* **22**, 782 (1969).
- ²²T. C. McGlinn, T. N. Krabach, M. V. Klein, G. Bajor, J. E. Greene, B. Kramer, S. A. Barnett, A. Lastras, and S. Gorbatskin, *Phys. Rev. B* **33**, 8396 (1986).
- ²³H. Bilz and W. Kress, in *Phonon Dispersion Relations in Insulators* (Springer-Verlag, Berlin, 1979).
- ²⁴A. S. Barker, Jr. and A. J. Sievers, *Rev. Mod. Phys.* **47**, 51 (1975), and references therein.
- ²⁵B. Champagnon, B. Andriansolo, and F. Duval, *J. Chem. Phys.* **94**, 5237 (1991).
- ²⁶R. Beserman, *Ann. Phys. (N.Y.)* **4**, 197 (1969), and references therein.
- ²⁷L. Genzel and T. P. Martin, *Phys. Status Solidi B* **51**, 91 (1972).
- ²⁸L. Wolf, S. B. Stanely, and K. A. McCarty, *American Institute Handbook of Physics* (McGraw-Hill, New York, 1963), p. 24.
- ²⁹R. Ruppini, *J. Phys. C* **8**, 1969 (1975), and references therein.
- ³⁰S. Hayashi and K. Yamamoto, *Phase Transit.* **24-26**, 641 (1990), and references therein.
- ³¹AL. L. Efros, A. I. Ekimov, F. Kozlowski, V. Petrova-Koch, H. Schimidbaur, and S. Shumilov, *Solid State Commun.* **78**, 852 (1991).